

Evolution of Convection During Tropical Cyclogenesis

David J. Raymond and Sharon L. Sessions
Physics Department and Geophysical Research Center
New Mexico Tech
Socorro, NM 87801 USA

December 1, 2006

Abstract

Central to tropical cyclogenesis is the changing behavior of moist convection as the cyclone evolves. Based on a cumulus ensemble model run in weak temperature gradient mode, we suggest that the mid-level vortex created by early-stage convection stabilizes the environment in way that favors further development. In particular, modeled convection occurring in the more stable environment produces heavy rainfall and concentrated inflow at low levels. Such inflow is needed for the development of the low-level vortex characteristic of warm-core tropical cyclones. The increase in humidity which is typical of developing cyclones also increases convective rainfall, but it does not act to concentrate the inflow at low levels.

1 Introduction

Under normal conditions deep convection over warm tropical oceans typically has its maximum vertical mass flux in the upper troposphere, implying that inflow is distributed through a deep layer (Yanai et al. 1973; Frank and McBride 1989; Mapes and Houze 1993, 1995). Furthermore, downdrafts produced by this convection often cause outflow in the lowest levels. The typical net convective inflow profile seen in this case acts through the circulation theorem to enhance vorticity preferentially at middle levels (Simpson et al. 1997). This type of convection is often concentrated in the active regions of cold core tropical waves.

We do not yet understand how a warm core cyclone develops out of such a wave. In particular, the mechanism by which a disturbance with cyclonic vorticity concentrated at mid-levels is converted into a system with a strong low-level circulation remains uncertain. This question is important because the heat flux produced by the

associated low-level winds is a key element in the thermodynamic engine of tropical cyclones (Emanuel 1988).

On the basis of an idealized model, Emanuel (1989) hypothesized that shallow, nonprecipitating convection serves to moisten mid-levels to the point that convective downdrafts are suppressed, resulting in low-level net convergence and spinup. Observations from TEXMEX (Tropical Experiment in Mexico; Bister and Emanuel 1997; Raymond et al. 1998) revealed a rather different picture. Though moistening of middle levels by convection increases the mid-level moist entropy to a certain degree, the decisive effect is the reduction of moist entropy at low levels. This diminishes the negative vertical gradient of moist entropy in the lower troposphere, and thus the presumed strength of downdrafts driven by the evaporation of rain. This should enhance net inflow at low levels, and hence result in more low-level spinup. Airborne Doppler radar observations from TEXMEX did indeed show a progressive lowering of the level of nondivergence (i. e., the level of maximum vertical mass flux) and a concentration of the inflow at low levels as cyclone precursors intensified (Raymond et al. 1998).

An alternative perspective on cyclogenesis was developed by Simpson et al. (1997), who noted that the low-level vortex appears to develop in conjunction with the merger of two or more mid-level mesoscale vortices and the subsequent axisymmetrization and intensification of the combined system. However, their numerical simulations suggest that the dry adiabatic dynamics of vortex merger is insufficient by itself to produce a low-level vortex; moist convection is involved in some (unspecified) way.

Hendricks et al. (2004) simulated the formation of a tropical cyclone using a high-resolution numerical model, and found that strong, rotating convective systems, which they called “vortical hot towers”, formed lower tropospheric vortices which then merged to produce the tropical cyclone vortex. In a sequel to this paper, Montgomery et al. (2006) performed idealized simulations of convection within a region dominated by an idealized mid-level mesoscale vortex in order to understand the spinup and merger process. The vortical hot towers in this case produced strong net convergence at low levels (≤ 2 km) in spite of the generation of significant downdrafts and cold pool production. As would be expected, spinup into a simulated tropical storm did indeed occur in this environment. However, the reasons for the confinement of convective inflow to low levels in this case are still not clear. Whether this is related to stabilization by rotation, as asserted by Hendricks et al. (2004), or whether it is due to the thermodynamic environment provided by the assumed vortex remains to be determined.

It is evident that we need to learn more about how convection interacts with the environment of a developing tropical cyclone. Regions of heavy rain in the tropics tend to have environments which are both moister and more stable than in less disturbed areas (Ramage 1971; McBride and Frank 1999). The moisturization and stabilization are likely due to the convection itself, so non-linear feedbacks are involved in this process. Such a modification of the convective environment is indeed seen in

easterly waves and other tropical synoptic-scale disturbances (Reed and Recker 1971; Thompson et al. 1979; Cho and Jenkins 1987).

We first outline the use of a numerical cloud model in weak temperature gradient (WTG) mode (Sobel and Bretherton 2000; Sobel et al. 2001; Derbyshire et al. 2004; Mapes 2004; Raymond and Zeng 2005) to follow the evolution of convection in the environment characteristic of an intensifying tropical disturbance. We then demonstrate that the evolving conditions in cyclogenetic regions foster increasing rainfall efficiency. In addition, the stabilization of the environment results in a shallower inflow layer which enhances the low-level vorticity convergence needed for tropical cyclogenesis.

2 Method

A useful measure of precipitation efficiency in moist convection is the gross moist stability (GMS; Neelin and Held 1987), which is defined as the ratio of the lateral export of moist entropy (or moist static energy) from a convective region to the mass flowing through the region. Ignoring irreversible entropy generation, the exported entropy equals the entropy source due to latent and sensible surface heat fluxes and radiation in a steady state. These two factors together we consider to constitute the thermodynamic forcing of convection. The smaller the GMS, the higher is the precipitation efficiency.

A variation on the GMS is the normalized gross moist stability (NGMS), which is the ratio of the laterally exported entropy to the laterally imported water vapor. The latter equals the rainfall minus the surface evaporation in a steady state, so the NGMS relates thermodynamic forcing directly to precipitation rate, which makes it a useful tool for understanding the control of precipitation by the environment (Raymond 2000).

We define the dimensionless NGMS in a region as

$$\gamma \equiv -\frac{T_R \overline{\nabla \cdot (\mathbf{u}s)}}{L \overline{\nabla \cdot (\mathbf{u}r)}} = \frac{T_R \delta s}{L \delta r} \quad (1)$$

where δs is the mean gain in the moist entropy of air flowing through a convective region and δr is the mean loss of water vapor. The constants T_R and L are a reference temperature and the latent heat of condensation. The overbar combines a horizontal integral over the region of interest and a vertical pressure integral over the depth of the troposphere. The variable \mathbf{u} is the horizontal wind, s is the specific moist entropy, r is the water vapor mixing ratio, and ∇ is the horizontal divergence operator.

Figure 1 illustrates some of the factors controlling the NGMS. We note that $\delta s = s_{out} - s_{in}$ and $\delta r = r_{in} - r_{out}$ where s_{in} , s_{out} , r_{in} , and r_{out} are the average values of moist entropy and water vapor mixing ratio flowing in and out of the convective system. In addition, $M\delta s = A(F_{es} - F_{et})$ and $M\delta r = A(R - F_{rs})$ in a steady state,

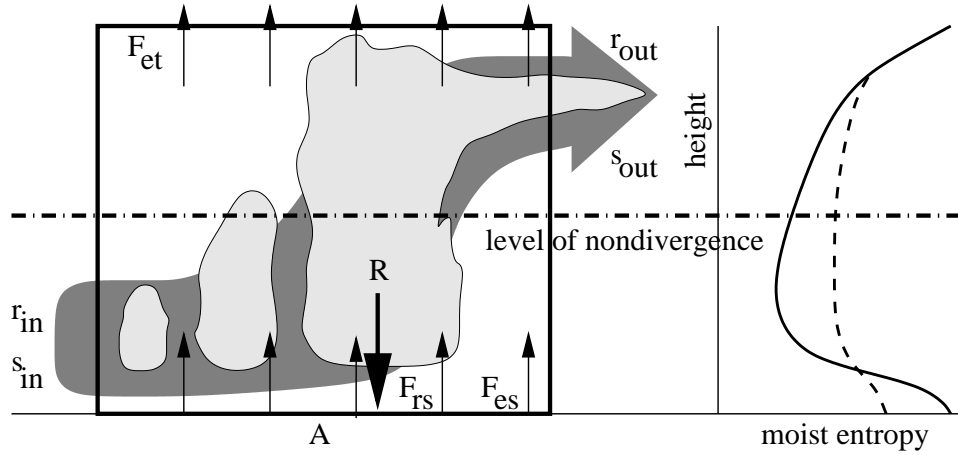


Figure 1: Factors controlling the NGMS. The quantities r_{in} and s_{in} are the water vapor mixing ratio and moist entropy entering the control volume (large rectangle), while r_{out} and s_{out} are the values of these quantities leaving the volume. Surface and tropopause fluxes of moist entropy are F_{es} and F_{et} and the surface evaporative flux and rainfall rate are F_{rs} and R . The horizontal area of the control volume is A . The solid moist entropy profile is typical of normal tropical conditions, while the dashed profile is characteristic of more disturbed conditions.

where F_{es} and F_{et} are the upward entropy fluxes at the surface and tropopause, R and F_{rs} are the rainfall and surface evaporation rates, A is the horizontal area of the control volume, and M is the mass of air per unit time flowing through this volume.

The level of nondivergence separates vertically the inflow from the outflow, and its level strongly influences the values of s_{in} and s_{out} in these currents, and hence the value of δs . In particular, the higher the level of nondivergence, the larger s_{out} will be relative to s_{in} , since the inflow will contain a large fraction of low entropy mid-level air. This results in a larger value of δs , and hence NGMS. Mass flux profiles with a lower level of nondivergence will be associated with correspondingly larger values of s_{in} , due to the smaller fraction of mid-level air in the inflow, and correspondingly smaller values of s_{out} , resulting in smaller δs . More stable moist entropy profiles, as represented by the dashed profile in figure 1, result in smaller δs under all circumstances, with a corresponding decrease in NGMS.

The NGMS is estimated using a cumulus ensemble model run in weak temperature gradient mode (Sobel and Bretherton 2000; Sobel et al. 2001; Raymond and Zeng 2005). In this model the lateral boundary conditions are periodic. However, the net effects of non-periodic (i.e., large-scale) flow over the domain are simulated by including additional sink terms E_e and E_r in the governing equations for specific moist entropy and water vapor mixing ratio. These terms are engineered to drive the mean vertical profile of virtual temperature toward a specified reference profile. This relaxation may be visualized as being the result of a mean vertical velocity

profile which produces cooling via upward advection of potential temperature so as to counter the heating associated with condensation and radiation in the model. We call this the WTG vertical velocity w_{wtg} . This velocity also advects moisture and moist entropy vertically. In addition, the horizontal divergence implied by mass continuity draws reference profile moisture and entropy into the computational domain when the divergence is negative. The sink terms may be related directly to the components of the NGMS: $\overline{E}_e = \overline{\nabla \cdot (\mathbf{u}s)}$ and $\overline{E}_r = \overline{\nabla \cdot (\mathbf{u}r)}$, so that

$$\gamma = -\frac{T_R \overline{E}_e}{L \overline{E}_r}. \quad (2)$$

Thus, for a specified reference profile, radiative model, and imposed surface wind speed (to generate surface fluxes), the model is run for a period of time and the NGMS is calculated from the time-averaged values of \overline{E}_e and \overline{E}_r .

The simulations reported here are nearly identical to those presented by Raymond and Zeng (2005). In particular, the model simulations are made on a small (50 km by 20 km) two-dimensional domain with 500 m by 250 m grid cells. Extension to a larger two-dimensional domain does not have a significant effect on the NGMS calculations. Three-dimensional calculations may yield somewhat different quantitative results, but are not expected to alter the general trends. The differences from Raymond and Zeng (2005) are as follows: (1) The simplified radiation scheme of Raymond (2001) is used in place of fixed radiative cooling. (2) Instead of a fixed reference profile in radiative-convective equilibrium, variations on the radiative-convective profile which increase the tropospheric moisture and decrease the static stability are employed.

Simulations were run for 2×10^6 s (≈ 23 d), with the NGMS calculated for conditions averaged over the second half of the simulations. The long averaging intervals are needed to obtain statistically stable results for the small domains used and discarding the first half of the simulations eliminates initial transients.

3 Results

Two sets of numerical experiments were performed to test the response of convection and the corresponding evolution of NGMS to conditions occurring in developing tropical storms. In each case, the control runs used unmodified radiative-convective equilibrium (RCE) profiles of potential temperature and moisture as the reference profiles in the weak temperature gradient mode. The RCE profiles were obtained with an imposed horizontal wind normal to the two-dimensional plane of the model of 5 m s^{-1} , and is considered to represent the environment far from the cyclone. In the first set of experiments, the RCE potential temperature profile was perturbed to increase atmospheric stability (warming at upper levels with cooling below) in order to represent the mean potential temperature profile inside a cyclone, while leaving the moisture profile unchanged. The second set of experiments used the RCE profile of potential temperature while increasing the moisture in the lower troposphere.

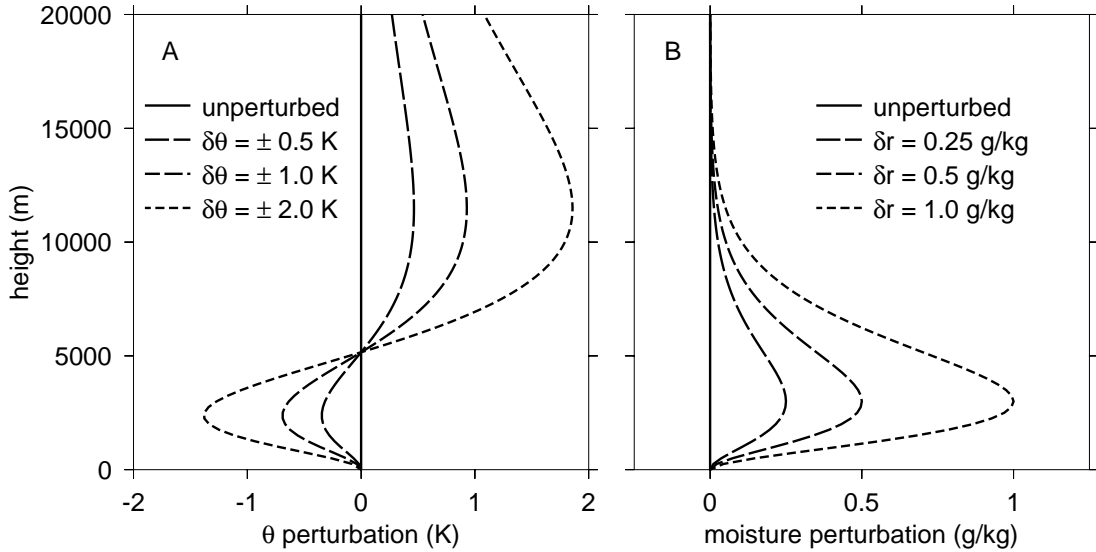


Figure 2: Profiles of (a) potential temperature perturbation and (b) mixing ratio perturbation used in the test cases.

For the first set of experiments we imposed a cooling of $\delta\theta$ centered at $h = 3$ km and a warming of the same magnitude centered at $h = 10$ km. Our assumed profiles are based on observations taken in a wide variety of convectively disturbed tropical environments. The perturbation centered at level h is of the form

$$\Delta\theta = \delta\theta \left(\frac{z}{h}\right)^2 e^{[2(1-z/h)]}, \quad (3)$$

where z is the height. We used $\delta\theta = \pm 0.5, 1.0,$ and 2.0 K, where the “+” corresponds to warming in the upper troposphere, the “−” indicates cooling at lower levels. The total perturbation is the sum of the two perturbations, and is shown in the left panel of figure 2. For the second set of experiments an additive perturbation of the mixing ratio r was made using (3) with $\Delta\theta$ replaced by the mixing ratio perturbation, $h = 3$ km, and $\delta r = 0.25, 0.5, 1.0$ g kg^{−1} replacing $\delta\theta$. The mixing ratio perturbation profiles are illustrated in the right panel of figure 2.

For each of the perturbation profiles shown in figure 2, simulations at different imposed horizontal wind speeds were performed to simulate increasing surface fluxes. The resulting rainfall rate and NGMS as a function of wind speed for selected values of $\delta\theta$ and δr are shown in figure 3.

The unperturbed runs are similar to the results of Raymond and Zeng (2005), and the perturbations show the response of rainfall rate and NGMS to an increase in reference atmospheric stability or mixing ratio. The overall effect of stabilizing the troposphere compared to radiative convective equilibrium is a decrease in NGMS and an increase in the rainfall rate. At low wind speeds, the decrease in NGMS and the increase in rainfall are quite dramatic, though the effect becomes fractionally less

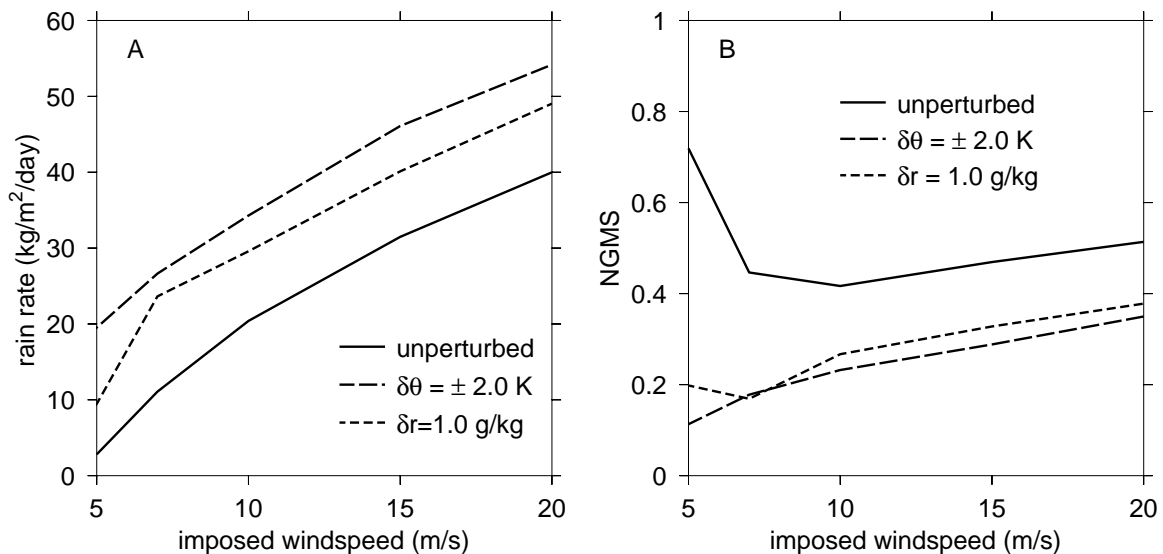


Figure 3: Rain rate (a) and NGMS (b) as a function of imposed horizontal wind speed for selected values of $\delta\theta$ and δr .

important at higher wind speeds. An increase in mixing ratio causes similar changes in the rainfall rate and NGMS.

Given the observed dependence of rainfall rate on saturation fraction, the increased rainfall rate due to a mixing ratio perturbation is as expected. However, the rainfall increase with increased stability is perhaps somewhat surprising. To understand this behavior, we examine the vertical mass flux profiles. A representative data set is shown in figure 4 for a horizontal imposed wind speed of 7 m s^{-1} . The most striking feature of these results is that increasing the atmospheric stability decreases the level of nondivergence from about 10000 m to 5000 m. These results are consistent with those seen in the convective simulations of Bretherton and Smolarkiewicz (1989). The lowering of the level of nondivergence is a feature that is more pronounced at lower wind speeds, and coincides with the sharp decrease in NGMS seen under these conditions. As explained earlier, these results are linked because lowering this level causes a decrease in δs and a resulting decrease in NGMS.

In the second set of experiments the increasing moisture also results in an increase in rainfall and a decrease in NGMS. However, as figure 4 shows, the level of nondivergence does not decrease significantly in this case. The decrease in δs and hence in NGMS is due totally to the increase in the value of s_{in} resulting from the increase in moisture at low levels.

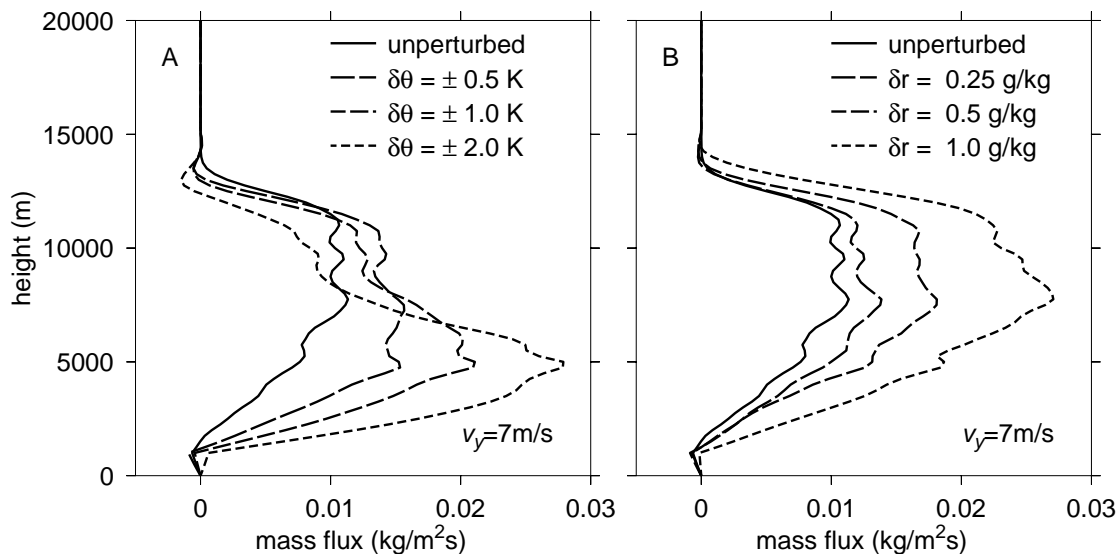


Figure 4: Time-averaged vertical mass flux profiles for an imposed horizontal wind-speed of 7 m s^{-1} . (a) Simulations with θ perturbations and (b) simulations with r perturbations.

4 Conclusions

As noted by Raymond et al. (1998), the spinup of a tropical cyclone depends ultimately on the balance between low-level vorticity convergence and surface friction. More intense rainfall implies more low to middle level mass convergence. The lower the level of nondivergence, the more this inflow is concentrated near the surface, resulting in increased vorticity at low levels. Enhanced vorticity implies stronger circulating wind speeds near the surface and more intense surface moist entropy fluxes. These fluxes drive more precipitation, resulting in positive feedback favoring further intensification. The strength of this feedback relative to the dissipative effects of surface friction determines whether the cyclone precursor disturbance intensifies.

Our numerical results show that a moistening of the column in the region of deep convection produces more rainfall per unit surface moist entropy flux. However, the stabilization of the column also has this effect and in addition results in a concentration of the inflow into a shallower layer, which produces more low-level vorticity convergence per unit rainfall. It is thus even more effective than moisturization in aiding the spinup of a tropical cyclone according to our simulations.

These results highlight the significance of the lowering of the level of nondivergence seen in developing tropical cyclones during TEXMEX. Our results suggest that this effect is due more to the stabilization of the environment than to its moistening.

This paper considers only the initial stage of the evolution of a tropical wave disturbance into a cyclone in which temperature and moisture anomaly profiles intensify but don't change shape. Limited evidence (Mapes and Houze 1995, Bister

and Emanuel 1997) suggests that the top of the low-level cold anomaly decreases in elevation as the system evolves. We speculate that this would cause the convective inflow layer to become even shallower, thus further aiding cyclogenesis.

Acknowledgments. This work was supported by National Science Foundation grant ATM-0352639.

5 References

- Bister**, M., and K. A. Emanuel, 1997: The genesis of hurricane Guillermo: TEXMEX analyses and a modeling study. *Mon. Wea. Rev.*, **125**, 2662-2682.
- Bretherton**, C. S., M. E. Peters, and L. E. Back, 2004: Relationships between water vapor path and precipitation over the tropical oceans. *J. Climate*, **17**, 1517-1528.
- Bretherton**, C. S., and P. K. Smolarkiewicz, 1989: Gravity waves, compensating subsidence and detrainment around cumulus clouds. *J. Atmos. Sci.*, **46**, 740-759.
- Cho**, H.-R., and M. A. Jenkins, 1987: The thermal structure of tropical easterly waves. *J. Atmos. Sci.*, **44**, 2531-2539.
- Derbyshire**, S. H., I. Beau, P. Bechtold, J.-Y. Grandpeix, J.-M. Piriou, J.-L. Redelsperger, and P. M. M. Soares, 2004: Sensitivity of moist convection to environmental humidity. *Quart. J. Roy. Meteor. Soc.*, **130**, 3055-3079.
- Emanuel**, K. A., 1988: The maximum intensity of hurricanes. *J. Atmos. Sci.*, **45**, 1143-1155.
- Emanuel**, K. A., 1989: The finite-amplitude nature of tropical cyclogenesis. *J. Atmos. Sci.*, **46**, 3431-3456.
- Frank**, W. M., and J. L. McBride, 1989: The vertical distribution of heating in AMEX and GATE cloud clusters. *J. Atmos. Sci.*, **46**, 3464-3478.
- Hendricks**, E. A., M. T. Montgomery, and C. A. Davis, 2004: The role of "vortical" hot towers in the formation of tropical cyclone Diana (1984). *J. Atmos. Sci.*, **61**, 1209-1232.
- Lucas**, C., E. J. Zipser, and B. S. Ferrier, 2000: Sensitivity of tropical west Pacific oceanic squall lines to tropospheric wind and moisture profiles. *J. Atmos. Sci.*, **57**, 2351-2373.
- Mapes**, B. E., 2004: Sensitivities of cumulus-ensemble rainfall in a cloud-resolving model with parameterized large-scale dynamics. *J. Atmos. Sci.*, **61**, 2308-2317.

- Mapes**, B., and R. A. Houze, Jr., 1993: An integrated view of the 1987 Australian monsoon and its mesoscale convective systems. II: Vertical structure. *Quart. J. Roy. Meteor. Soc.*, **119**, 733-754.
- Mapes**, B., and R. A. Houze, Jr., 1995: Diabatic divergence profiles in western Pacific mesoscale convective systems. *J. Atmos. Sci.*, **52**, 1807-1828.
- McBride**, J. L., and W. M. Frank, 1999: Relationships between stability and monsoon convection. *J. Atmos. Sci.*, **56**, 24-36.
- Montgomery**, M. T., M. E. Nicholls, T. A. Cram, and A. B. Saunders, 2006: A vortical hot tower route to tropical cyclogenesis. *J. Atmos. Sci.*, **63**, 355-386.
- Neelin**, J. D., and I. M. Held, 1987: Modeling tropical convergence based on the moist static energy budget. *Mon. Wea. Rev.*, **115**, 3-12.
- Ramage**, C. S., 1971: *Monsoon meteorology*. Academic Press, New York, 296 pp.
- Raymond**, D. J., 2000: Thermodynamic control of tropical rainfall. *Quart. J. Roy. Meteor. Soc.*, **126**, 889-898.
- Raymond**, D. J., 2001: A new model of the Madden-Julian oscillation. *J. Atmos. Sci.*, **58**, 2807-2819.
- Raymond**, D. J., C. López-Carrillo, and L. López Cavazos, 1998: Case-studies of developing east Pacific easterly waves. *Quart. J. Roy. Meteor. Soc.*, **124**, 2005-2034.
- Raymond**, D. J., and X. Zeng, 2005: Modelling tropical atmospheric convection in the context of the weak temperature gradient approximation. *Quart. J. Roy. Meteor. Soc.*, **131**, 1301-1320.
- Reed**, R. J. and E. E. Recker, 1971: Structure and properties of synoptic-scale wave disturbances in the equatorial western Pacific. *J. Atmos. Sci.*, **28**, 1117-1133.
- Simpson**, J., E. Ritchie, G. J. Holland, J. Halverson, and S. Stewart, 1997: Mesoscale interactions in tropical cyclogenesis. *Mon. Wea. Rev.*, **125**, 2643-2661.
- Sobel**, A. H., and C. S. Bretherton, 2000: Modeling tropical precipitation in a single column. *J. Climate*, **13**, 4378-4392.
- Sobel**, A. H., J. Nilsson, and L. M. Polvani, 2001: The weak temperature gradient approximation and balanced tropical moisture waves. *J. Atmos. Sci.*, **58**, 3650-3665.
- Thompson**, R. M., S. W. Payne, E. E. Recker and R. J. Reed, 1979: Structure and properties of synoptic-scale wave disturbances in the intertropical convergence zone of the eastern Atlantic. *J. Atmos. Sci.*, **36**, 53-72.

Yanai, M., S. Esbensen and J. H. Chu, 1973: Determination of bulk properties of tropical cloud clusters from large scale heat and moisture budgets. *J. Atmos. Sci.*, **30**, 611-627.